

DFT investigation of methane metathesis with L2AnCH3 actinide complexes catalysts (L = Cl, Cp, Cp*; An = Ac, Th, Pa, U, Np, Pu)

F. Talbi-Ingrachen, F. Talbi, F. Kias, A. Elkechai, A. Boucekkine, C. Daul

▶ **To cite this version:**

F. Talbi-Ingrachen, F. Talbi, F. Kias, A. Elkechai, A. Boucekkine, et al.. DFT investigation of methane metathesis with L2AnCH3 actinide complexes catalysts (L = Cl, Cp, Cp*; An = Ac, Th, Pa, U, Np, Pu). Computational and Theoretical Chemistry, 2018, 1138, pp.123-134. 10.1016/j.comptc.2018.06.009 . hal-01835015

HAL Id: hal-01835015

https://univ-rennes.hal.science/hal-01835015

Submitted on 13 Jul 2018

HAL is a multi-disciplinary open access archive for the deposit and dissemination of scientific research documents, whether they are published or not. The documents may come from teaching and research institutions in France or abroad, or from public or private research centers.

L'archive ouverte pluridisciplinaire **HAL**, est destinée au dépôt et à la diffusion de documents scientifiques de niveau recherche, publiés ou non, émanant des établissements d'enseignement et de recherche français ou étrangers, des laboratoires publics ou privés.

ACCEPTED MANUSCRIPT

DFT investigation of methane metathesis with L_2AnCH_3 actinide complexes catalysts (L = Cl, Cp, Cp*; An = Ac, Th, Pa, U, Np, Pu).

Fazia Talbi-Ingrachen[a,b], Fatiha Talbi[b], Farida Kias[b],

Aziz Elkechai[b*], Abdou Boucekkine[c*], Claude Daul[d]

[a]*Laboratoire de Physicochimie Théorique et Chimie Informatique, Faculté de chimie, USTHB, Bab Ezzouar, BP 32 El Alia, Alger, Algeria*

[b]*Laboratoire de Physique et Chimie Quantique, Faculté des Sciences, Université Mouloud Mammeri de Tizi-Ouzou, BP 17 RP 15000, Algeria*

[c]*Univ Rennes, CNRS, ISCR - UMR 6226, F-35000 Rennes, France*

[d]*Laboratoire de Chimie Computationnelle, Université de Fribourg, Chemin du musée 9 CH-1700 Fribourg, Switzerland*

*** Corresponding Authors:**

E-mail: A.E.: azizelkechai@yahoo.fr; aziz.elkechai@ummto.dz

A.B.: abdou.boucekkine@univ-rennes1.fr

ACCEPTED MANUSCRIPT

Abstract

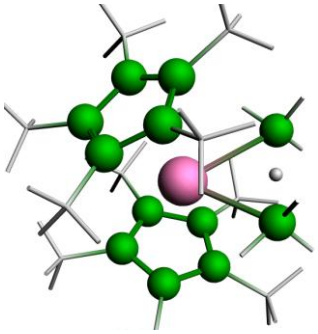
In order to understand the catalytic activity of the actinide complexes L_2AnCH_3 (An = Ac, Th, Pa, U, Np and Pu; L = Cl, Cp and Cp*) towards the activation of the C–H bond of methane, relativistic ZORA/DFT investigations have been carried out. The results obtained from Linear Transit (LT) and Intrinsic Reaction Coordinate (IRC) calculations show that the mechanism involved in these reactions starts with a proton transfer from methane to the methyl group of the complex leading to the formation of a four center transition state characteristic of a bond metathesis process. The U(III) and Np(III) complexes exhibit a high ability to activate the methane C–H bond, the activation energies being respectively equal to 10.5, 17.1 and 21.0 kcal/mol for Cl_2NpCH_3, Cp_2NpCH_3 and $Cp^*_2UCH_3$ respectively whereas the Th(III) complexes exhibit the highest activation energy, 34.9 kcal/mol for $Cp^*_2ThCH_3$. Since the initial step of the reaction is viewed as a proton transfer, the analysis of the charges evolution and frontier molecular orbitals of the complexes and the transition states, shows that a facile polarization of the bonds involved in the reaction has the effect of reducing the activation energy. The role of the metallic 5f orbitals in the reactivity of the L_2AnCH_3 compounds towards CH_4 is analyzed and discussed. More important the 5f actinide orbital contribution, less important is the activation energy.

Key-words: C–H bond activation, Actinide complexes, DFT calculations, Reaction mechanism.

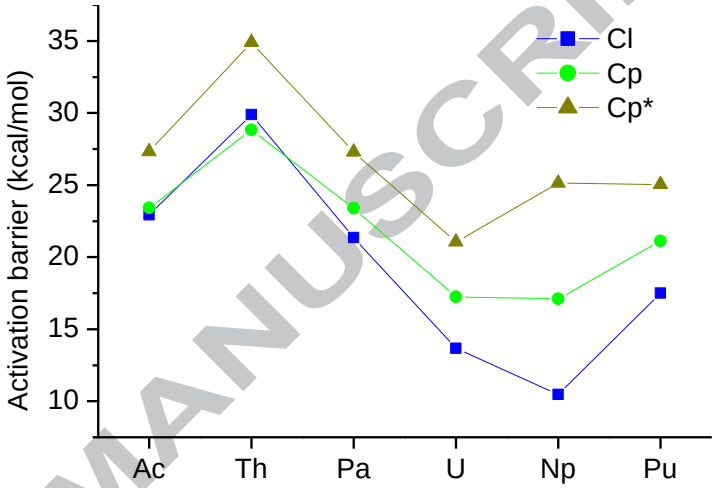
ACCEPTED MANUSCRIPT

ACCEPTED MANUSCRIPT

GRAPHICAL ABSTRACT



$Cp^*_2ThCH_3+CH_4$ Transition State



ACCEPTED MANUSCRIPT

ACCEPTED MANUSCRIPT

1. Introduction

The potential catalytic reactivity of metallic compounds leading to the functionalization of alkane C–H bonds [1–2] presents important applications in the chemical industry with financial and environmental benefits. It allows the conversion of saturated hydrocarbons into value–added chemicals products. Thus, such bonds activation by organometallic compounds has been an attracting and fascinating subject for a long time since the discovery of the role of the transition metal mediation in the activation of the C–H [3–7] as well as C–F [8–9], C–C, and H–H [10] strong bonds reminding their high bonding energy, about 100 kcal/mol for C–H. Among the pioneers in this area, Janowicz and Bergman [11] reported in 1982 the C–H additive–oxidative activation by the iridium complex $(Cp^*)(PMe_3)IrH_2$ in a high yield photolysis of a saturated hydrocarbon (R−H) solution at room temperature leading to the formation of the hydrido alkyl complex $(Cp^*)(PMe_3)Ir(R)(H)$. Since then, investigations were carried out, not only on the reactivity of the transition metal ions/complexes toward C–H bonds [12–16] but also on those involving f–block metal ones [17]. Thus, in 1983, Watson et al [18] showed the role of the $Lu(Cp^*)_2R$ (R = CH_3, H) complex mediation in the activation of various sp^2 and sp^3 C–H bonds as well as the sp^3 C–H bond of methane.

Activation of these inert bonds by organometallic complexes occurs via different modes like oxidative addition, 1,2–addition, σ–complex–assisted mechanism (σ–CAM) and electrophilic processes [19–21]. The mainly known and most common mode especially for C–H bond activation by lanthanide and actinide complexes is the sigma–bond metathesis which involves a four centers transition state without change of the metal oxidation state [22]. Indeed, using DFT/B3PW91 calculations for the study of the CH_4 activation by the $(Cp_2)^*LnMe$ complex where Cp^* is modeled by Cl and Ln is a lanthanide atom, Maron and coworkers [23] demonstrated that the overall reaction was sigma–bond metathesis which proceeds via proton transfer between two anionic groups near the lanthanide center [24].

Regarding actinide complexes, few experimental studies [25–26] and less theoretical studies related to the activation of C–H bonds have been reported [27]. The experimental investigation performed by Kiplinger and coworkers [28] highlighted the sp^3 and sp^2 C–H bonds activation by Th(IV) and U(IV) metallocene complexes respectively which were rationalized theoretically using DFT (B3LYP) computations by Yang et al [29]. Otherwise, the study of the reactivity of Ac^+–Pu^+ actinide cations toward methane C–H bond in gas phase, using a DFT approach, has been reported by Almeida et al [30].

In order to clarify the potential catalytic activity of different actinide complexes towards CH_4 C–H bond activation and the role of the various ligands, we have undertaken a DFT study of

ACCEPTED MANUSCRIPT

the reaction $L_2AnCH_3 + CH_4$ (L = Cl (chlorine), Cp (cyclopentadienyl), Cp* (pentamethylcyclopentadienyl); An = Ac, Th, Pa, U, Np, Pu). The analysis of the obtained results and the comparison with those involving lanthanide complexes should provide an understanding of the reaction process, the ability of the actinide complexes to activate the methane C–H bond as well as the role of the ligand (Cl, Cp et Cp*) on these reactions. The role of the 5f electrons of the actinide ions in the reaction will be also investigated.

2. Computational details

For all the studied complexes, the calculations were performed using Density Functional Theory (DFT) [31–33], scalar relativistic corrections being introduced via the zeroth–order regular approximation (ZORA) [34–36] to the Dirac equation. Solvent effects (tetrahydrofuran, THF) have been accounted using the conductor–like screening model (COSMO) [37], as implemented in the employed Amsterdam Density Functional (ADF2014.01) program package, which is well suited for the study of the electronic structure and reactivity of actinide molecular systems [38–40]. The Vosko–Wilk–Nusair functional (VWN) [41] for the local density approximation and the gradient corrections for the exchange and correlation of Becke and Perdew, respectively, i.e., the BP86 functional [42–43] have been used.

Geometry optimizations which have been carried out at the scalar relativistic level were followed by single point computations including spin–orbit coupling. In this work, we used for all atoms a triple–ζ Slater-type valence orbitals augmented by one set of polarization functions, *i.e.* the triple–zeta polarized (TZP) basis set, taken from the ADF/ZORA/TZP database directory. The spin unrestricted DFT formalism is used for the open–shell systems. The frozen–core approximation, where the core density is obtained from four component Dirac–Slater calculations, has been applied for all atoms; the electronic cores 1s and 1s/2s/2p were frozen for the elements carbon (C.1s) and chlorine (Cl.2p) respectively. The atomic basis sets of the heavy element An, include the valence 5f/6s/6p/6d/7s/7p shells, were considered according to the "medium core" approximation (An.5d). Numerous theoretical studies have shown that the ZORA/BP86/TZP approach reproduces the experimental geometries and ground–state properties of f–element complexes with a satisfying accuracy [44–47].

In this study, we carried out first the full geometry optimizations of the species under consideration, in the gas phase, at the spin unrestricted level. Next, the geometries were re–

ACCEPTED MANUSCRIPT

optimized in the solvent (THF) using the COSMO model. We used the non–default Delley type of cavity [37b], the solvent being considered with its relative dielectric constant of 7.58 and its effective cavity radius of 3.18 Å. Then, our complexes being f–element species, where spin−orbit corrections are expected to be important, single–point calculations including spin–orbit coupling were done using the previously optimized geometries, for both the gas phase and the solution.

Through an harmonic vibrational frequency analysis, the stationary points on the potential energy surface (PES) identified via linear transit (LT) calculations performed for all L_2AnCH_3 + CH_4 reactions, were confirmed to be equilibrium structures (all normal modes have real frequencies, NIMAG = 0), or transition states (TSs) characterized by one normal mode with an imaginary frequency (NIMAG = 1). The character of the normal mode associated with the imaginary frequency was analyzed to ensure that the correct transition state was found. The connectivity between the stationary points was established by intrinsic reaction coordinate (IRC) calculations [48] to check the connections of the first−order saddle points with the local minima found on the PES. The zero−point vibration energy (ZPVE) contributions have been included in the computed free energies at T = 298.15 K. The activation energies $\Delta G^{\#}$ are then calculated as the free energy differences between the transition state and the reactant ($\Delta G^{\#} = \Delta G(TS) - \Delta G(reactants)$), whereas the enthalpy barriers represent the enthalpy differences between the transition state and the reactant ($\Delta H^{\#} = \Delta H(TS) - \Delta H(reactants)$), and the electronic activation energies $\Delta E^{\#}$ corresponds to the total bonding energies (TBEs) differences ($\Delta E^{\#} = TBE(TS) - TBE(reactants)$) between the transition state and the reactants, reminding that the ADF program computes TBEs of the considered species instead of their energies.

Finally, the Mulliken populations and Hirshfeld analyses were carried out to follow the charge transfers during the chemical reactions.

The computational exploration of f–block element compounds reactivity is a difficult task owing to the fact that it often involves open shell systems, with spin contamination and SCF convergence problems. It should be noted that in our case, we checked that all species occurring during the L_2AnCH_3 + CH_4 reaction process (reactants, TSs and products) exhibit a negligible spin contamination (deviation less than 3% between the computed values $<S^2>$ of the squared spin operator and the exact ones).

ACCEPTED MANUSCRIPT

3. Results and discussion

3.1. Preliminary calculations

In order to verify the reliability of the methodology used in the present work, the C–H bond activation by actinide complexes $(Cp)_2An(Me)_2$ with An = U and Np have been explored in order to compare our results to the previous studies involving the same complexes and the same reactions [49]. In these studies, Castro et al. used a DFT approach with the B3PW91 functional validated by CASSCF (complete active space SCF) computations. The same methodology was used by Barros et al. [50] to the study of the reaction of Cp_2UNMe and Cp_2UO with MeC≡CMe and H_3Si–Cl. By comparing the results obtained with the multireference calculations (CAS (2,7) for U and CAS (3,7) for Np) to those obtained by DFT approach, the authors observed that these systems do not exhibit significant multireference character, only one configuration is dominant with a weight practically equal to 100 %

The obtained results using our (ZORA/BP86) approach on $(Cp)_2An(Me)_2$ complexes are reported on Figure 1 where the structures of the reactants and TSs are displayed. Concerning the reactivity of $(Cp)_2U(Me)_2$ with methane as well as the reaction involving $(Cp)_2Np(Me)_2$, the geometrical parameters of the reactant and the TS are in good agreement with those obtained by Castro et al. (Geometrical coordinates are given in SI 1). As it can be seen, the calculated U–C2 bond lengths in the reactant and TS are 2.40 and 2.60 Å respectively, close to those of Castro and coworkers, respectively 2.40 and 2.65 Å. The activation energies $\Delta G^{\#}$ of the $Cp_2AnMe_2 + CH_4$ reaction with An = U and Np are found to be equal to 34.8 kcal/mol and 32.6 kcal/mol respectively whereas the previous study of Castro estimates these activation energies around 41.7 kcal/mol and 39.6 kcal/mol respectively, noting that the energy difference between the two actinide complexes is the same in both calculations.

To conclude, our ZORA/BP86 approach leads to very similar results to those previously published, and can then be used in the study of the reactivity of L_2AnCH_3 (L = Cl, Cp and Cp*) complexes toward the methane molecule.

ACCEPTED MANUSCRIPT

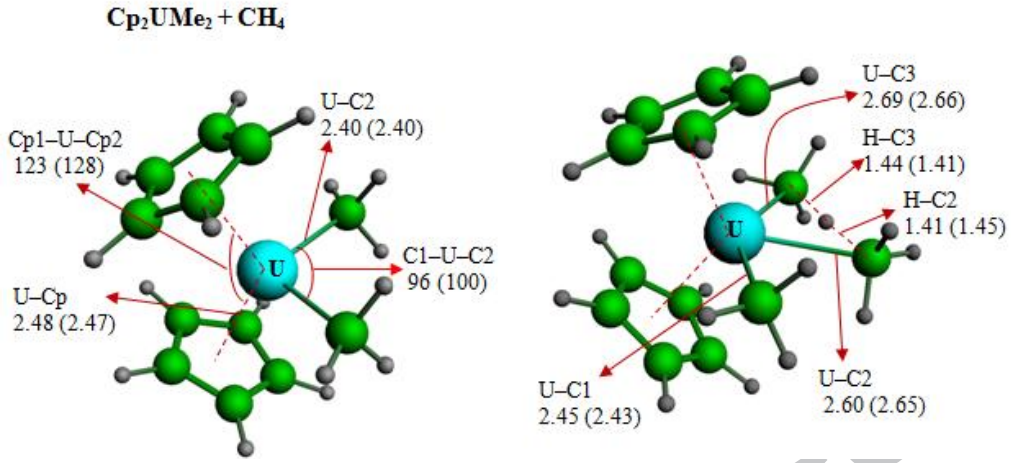


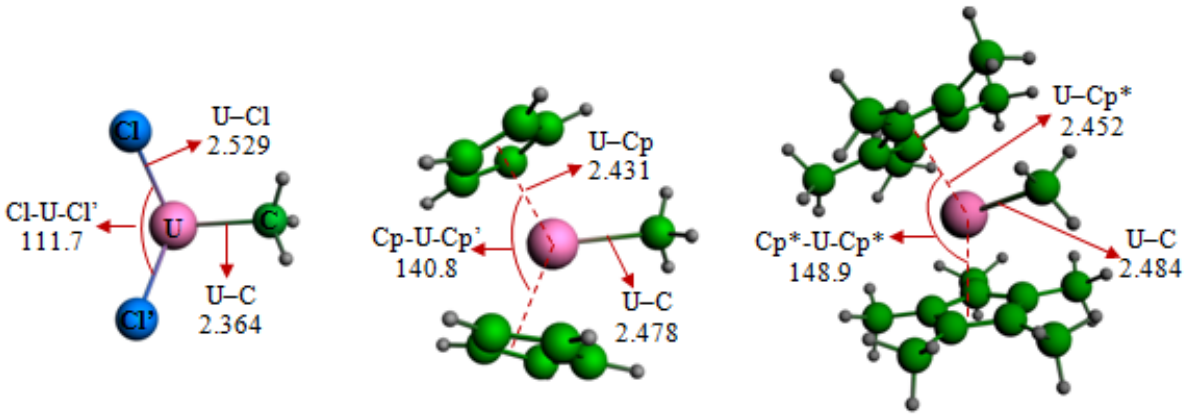
Fig. 1. Optimized geometries of the reactant and transition state for the reaction $Cp_2U(CH_3)_2$ + CH_4. Distances in angstroms (Å) and angles in degrees (°). Values of reference [49] between parentheses.

3.2. L_2AnCH_3 complexes

Optimized geometries

The geometries of the L_2AnCH_3 complexes where An = Ac, Th, Pa, U, Np, and Pu and L = Cl, Cp, and Cp* have been fully optimized in the gas phase and in the solvent THF, at the spin–unrestricted level of theory. All compounds were considered without any symmetry constraints. We have considered different possible spin states for each complex. The optimized geometries determined in both the gas phase and THF solvent have been verified as minima by vibration frequencies calculation.

The overall symmetry of the optimized structures has been found similar for all actinide complexes. As an example we display on Figure 2 the optimized geometries of the uranium complexes.



ACCEPTED MANUSCRIPT

Fig. 2. Optimized geometries of L_2UCH_3 complexes (with L = Cl, Cp and Cp*). Distances are in angstroms (Å) and angles in degrees (°).

The ground state optimized geometrical parameters of the Cl_2AnCH_3 and Cp_2AnCH_3 (with An = Ac, Th, Pa, U, Np and Pu) complexes are reported in Table 1.

Table 1: Main geometrical parameters[a] (distances (Å) and angles (°)) of An(III) L_2AnCH_3 complexes (L = Cl and Cp) at the ZORA/BP86/TZP level in gas phase.

Cl_2AnCH_3	Ac	Th	Pa	U	Np	Pu
An–Cl	2.685	2.590	2.544	2.529	2.531	2.535
An–C	2.538	2.404	2.349	2.364	2.363	2.359
Cl–An–Cl'	114.4	131.9	124.0	111.7	114.2	118.4
Sum of angles	324.0	358.7	341.8	312.7	312.2	315.2
Cp_2AnCH_3	Ac	Th	Pa	U	Np	Pu
An–Cp	2.688	2.554	2.447	2.431	2.465	2.471
An–Cp'	2.688	2.552	2.439	2.466	2.461	2.462
An–C	2.620	2.500	2.453	2.478	2.464	2.460
Cp–An–Cp'	138.6	137.6	126.7	140.8	134.1	127.7

[a]Distances and angles are defined in Fig. 2

In this series of complexes, the results show that the variation of the An–Cl distance is not equal to the contraction of the An(III) ionic radius. Indeed, the M–Cl distance decreases from Ac to U by 0.156 Å for an ionic contraction equal to 0.090 Å; the U–Cl, Np–Cl and Pu–Cl distances are calculated to be very close.

The observed differences do not exceed 6.10^{-3} Å for a contraction of the ionic radius equal to 0.033 Å. A slightly different trend is observed in the case of the An–C distance with the exception of the Cl_2PaCH_3 complex which has the smallest An–C bond (2.349 Å). A bond length shortening of 0.179 Å is observed going from Ac to Pu for a contraction of the ionic radius equal to 0.125 Å. However, like the An–Cl distances, the U–C, Np–C and Pu–C distances are very close; the calculated differences do not exceed 5.10^{-3} Å. This trend is in accordance with the Nalewajski–Mrozek (NM) bond orders [51] where the values of the An–Cl and An–C bond indices, increase from 1.023 to 1.303 and from 0.870 to 1.039 respectively, in accordance with the decrease of the corresponding distances from Ac to Pa, then these values decrease insignificantly until Np (1.234 and 0.999). Pu complex presents the lowest bond indices (0.648 and 0.738 respectively) (Full NM bond orders are in SI.6).

ACCEPTED MANUSCRIPT

The structures of Cl_2AnCH_3 complexes have more or less pyramidal geometries as indicated by the sum of the bond angles An–Cl and An–C, except the complex Cl_2ThCH_3 which has a planar triangular geometry as indicated by the value of the sum of its bonding angles (equal to 360 °).

In the case of Cp_2AnCH_3 complexes like their Cl_2AnCH_3 counterparts, the An–C distance decreases by 0.160 Å (against 0.179 Å in the Cl_2AnCH_3 complexes) going from Ac (2.620 Å) to Pu (2.460 Å), with the exception of Cp_2PaCH_3 complex which has the shortest distance An–C like its Cl_2PaCH_3 counterpart. It is noteworthy that this An–C distance is longer in the Cp_2AnCH_3 complexes compared to the Cl_2AnCH_3 complexes because of the steric hindrance of the Cp groups. The variation of the distances An–(Cp) and An–(Cp') where (Cp) indicates the center of the ring, does not follow also the contraction of the metallic ionic radius. Although they are both very close for all complexes, they do not vary exactly in the same way. The mean distance An–(Cp) decreases significantly from Ac to Pa by about 0.245 Å and then increases slightly to Pu by 0.024 Å. The (Cp)–An–(Cp') angle in Pa and Pu complexes is smaller; this is probably due to a steric repulsion effect between the two cyclopentadienyl ligands which is less important when the An–(Cp) distance is shorter, as in the case of Pa complex.

When the Cp ligand is substituted by the Cp* ligand, we note a very slight increase in the An–C distances. Its variation throughout the series of complexes remains unchanged. On the other hand, the Cp*–An–Cp* angle is greater than the Cp–An–Cp one with a maximum deviation equal to 23.9° in the case of the Pa complex. This is probably due to the steric hindrance effect due the methyl groups of the Cp*. The effect of the solvent on these neutral complexes is not important. There is only a slight decrease of the An–C (Cp*) distances. Indeed, with the exception of the Ac complex, the distance An–C(CH_3) increases by 0.02 Å. The angle Cp*–An–Cp* is almost invariant, the whole geometric parameters are given in SI.3.

Generally, the total bonding energies (TBEs) of Cl_2AnCH_3 complexes in their high spin ground states are of the same order of magnitude, although they decrease from the Ac complex (–31.521 eV) to the Np one (–34.640 eV) in accordance with the number of unpaired electrons, in other words with the number of 5f electrons. When the Cl ligand is substituted by the Cp or Cp* ligand, the TBE variation still remain the same in the two series of complexes.

The TBEs of all complexes, including the solvent effects and spin–orbit corrections are given in Table SI.5 as well as the discussion of these values.

ACCEPTED MANUSCRIPT

Charge and frontier molecular orbital (FMO) analysis

In order to investigate the electronic structure of the L_2AnCH_3 complexes, in particular the metal–ligand interactions, Mulliken populations (MPA) and Hirshfeld [52] charges analyses were carried out. For example, in Table 2 are given the net charges of the metal, the CH_3 group and Cl ligand of Cl_2AnCH_3 complexes as well as the metal spin population (MSP) which is given by the difference between the total spin populations α and β of the metal, for the Ac, Th, Pa, U, Np and Pu complexes.

Table 2: MPA, Hirshfeld atomic charges (values in parentheses) of Cl_2AnCH_3 in the gas phase.

An^{+3}	Spin population	Mulliken - (Hirshfeld) net charges		
		An	Cl_2	CH_3
Ac ($5f^0$)	0.00	1.29 (0.88)	–0.90 (–0.61)	–0.39 (–0.27)
Th ($5f^1$)	1.04	1.00 (0.61)	–0.67 (–0.43)	–0.32 (–0.18)
Pa ($5f^2$)	2.13	0.92 (0.64)	–0.64 (–0.45)	–0.28 (–0.19)
U ($5f^3$)	3.17	1.05 (0.66)	–0.73 (–0.46)	–0.32 (–0.20)
Np ($5f^4$)	4.20	1.05 (0.67)	–0.74 (–0.48)	–0.31 (–0.20)
Pu ($5f^5$)	5.27	1.10 (0.78)	–0.79 (–0.57)	–0.31 (–0.21)

The ligand–to–metal donation is evidenced by the net MPA charge of the metal, varying from 0.92 for Pa complex to 1.29 for Ac complex, which is much lower than its ionic charge +3. As indicated by the negative charge of the CH_3 fragments the metal–methyl bond exhibits some ionic character. A detailed charge analysis is reported in SI.6. Moreover, Hirshfeld analysis leads to lower net charges compared to MPA ones.

In order to highlight the role of the orbitals of the actinide atom, particularly that of the valence shell in the studied complexes, a frontier molecular orbital (FMO) analysis was undertaken. In particular, we will focus on the highest single occupied molecular orbital (SOMO or HOMO) and the lowest unoccupied molecular orbital (LUMO).

The FMO diagram of Cl_2AnCH_3 is displayed in Figure 3 (the full diagrams of all complexes with different ligands are given in SI.7). The energies of these FMOs are given with the percentages d/f/An/L representing the percentage weights of the d and f orbitals, as well as those of actinide atoms and all ligands L (L_2 + CH_3). All the FMOs of the Pa, U, Np and Pu complexes are of predominantly 5f metallic character with a minor contribution of the ligands

ACCEPTED MANUSCRIPT

in the first three complexes (less than or equal to 3.7%) and a significant contribution (10%) to the LUMO in the last complex.

The FMOs of Th complex are mainly localized on the metal atom. The contribution of the 5f orbitals is negligible in the SOMO (1.9%) and is important in the LUMO (52.4%). In the Cl_2AcCH_3 complex, the SOMO is delocalized on the metal center and the carbon of the methyl group with a greater participation of the latter (61.4%). The LUMO has a majority metallic character (92.3%).

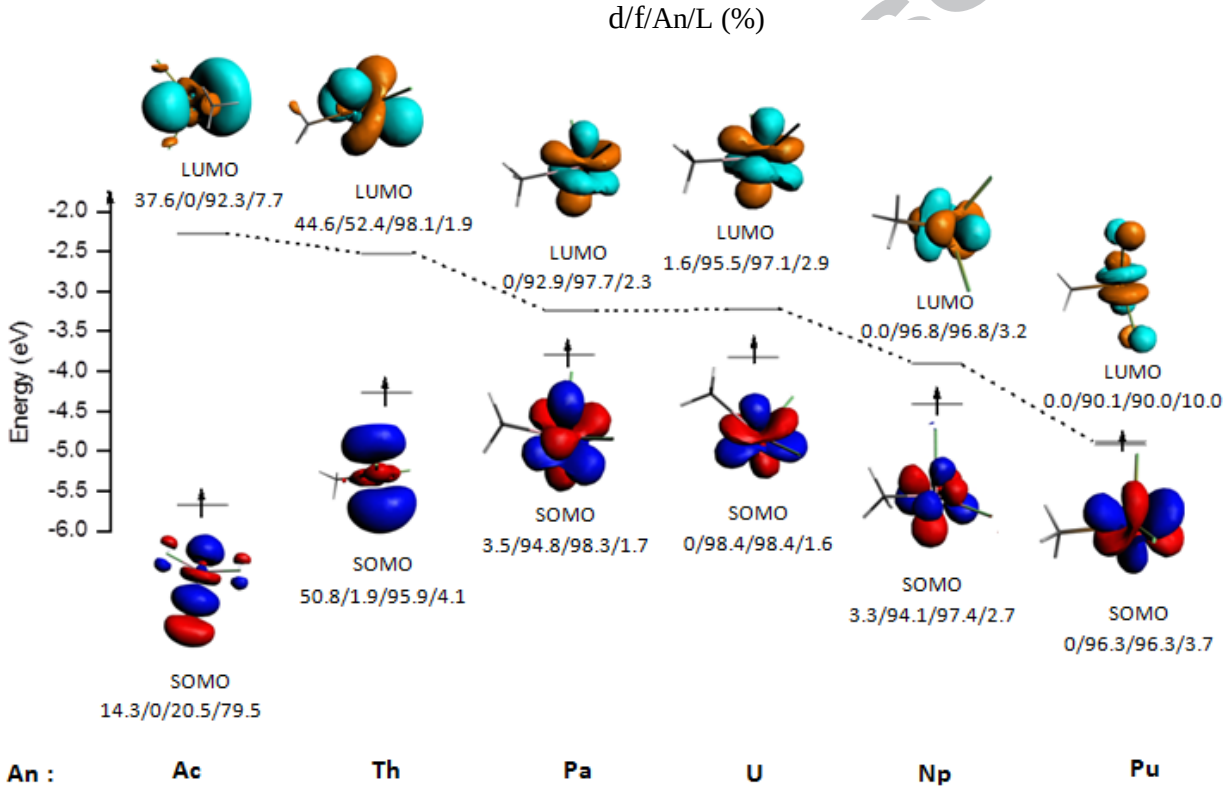


Fig. 3. Frontier Molecular Orbitals diagram of Cl_2AnCH_3 complexes at the ZORA/BP86/TZP level.

Like their Cl_2AnCH_3 counterparts, the FMOs of the Cp_2AnCH_3 and $Cp^*_2AnCH_3$ species with An = Pa, U, Np and Pu are localized on the metal and exhibit mainly a 5f character but this time with a lower contribution compared to Cl_2AnCH_3 complexes.

ACCEPTED MANUSCRIPT

3.3. Methane C–H bond activation by L_2AnCH_3 complexes

The activation reaction of the C–H bond of methane CH_4 by the actinide complexes was studied in the gas phase and in THF solution at the same level of theory, namely using DFT/ZORA/BP86/TZP calculations. The balance equations are given in scheme 1:

$$Cl_2AnCH_3 + \mathbf{CH_3}H \longrightarrow Cl_2An\mathbf{CH_3} + CH_4 \quad (1)$$

$$Cp_2AnCH_3 + \mathbf{CH_3}H \longrightarrow Cp_2An\mathbf{CH_3} + CH_4 \quad (2)$$

$$(Cp^*)_2AnCH_3 + \mathbf{CH_3}H \longrightarrow (Cp^*)_2An\mathbf{CH_3} + CH_4 \quad (3)$$

Scheme 1 (the bold blue color to indicate the transferred methyl group from methane to the complex)**.**

This reaction, also called Watson exchange, was observed for the first time with the complex $(Cp^*)_2Lu(III)Me$ [18]**.**

Transition state geometries

The linear transit (LT) approach was performed in order to identify the transition states on the PES for all reactions between L_2AnCH_3 (An = Ac, Th, Pa, U, Np and Pu; L= Cl, Cp, Cp*) and CH_4. The different spin states in our case of An(III) oxidation state are respectively singlet, doublet, triplet, quartet, quintet and sextet respectively for Ac, Th, Pa, U, Np and Pu complexes. All optimized TS structures have been identified as transition states by means of vibration frequency calculations which are characterized by the presence of one imaginary frequency for each TS which corresponds to a step towards C–H bond breaking (all TSs frequencies are given in SI.4). For instance, the vibration mode obtained at i1089.6 cm^{-1} in the case of the $Cl_2UCH_3 + CH_4$ reaction corresponds to the stretching of the C–H bond to form and break the two bonds $H_3C–H–CH_3$ involved in the reaction. The obtained results show that the optimized TS structures of all reactions (1, 2 and 3) have similar geometries and all exhibit a four–center cycle formed by An, C1, H4 and C2 atoms as displayed in Figure 4.

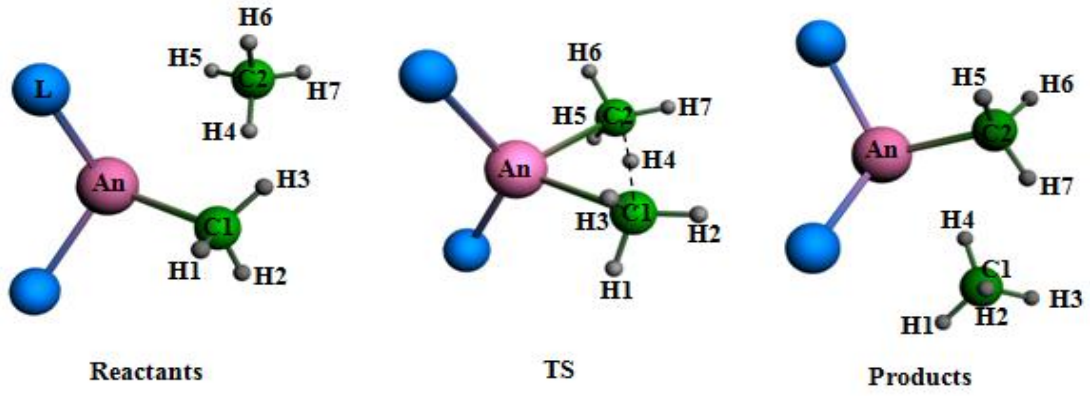
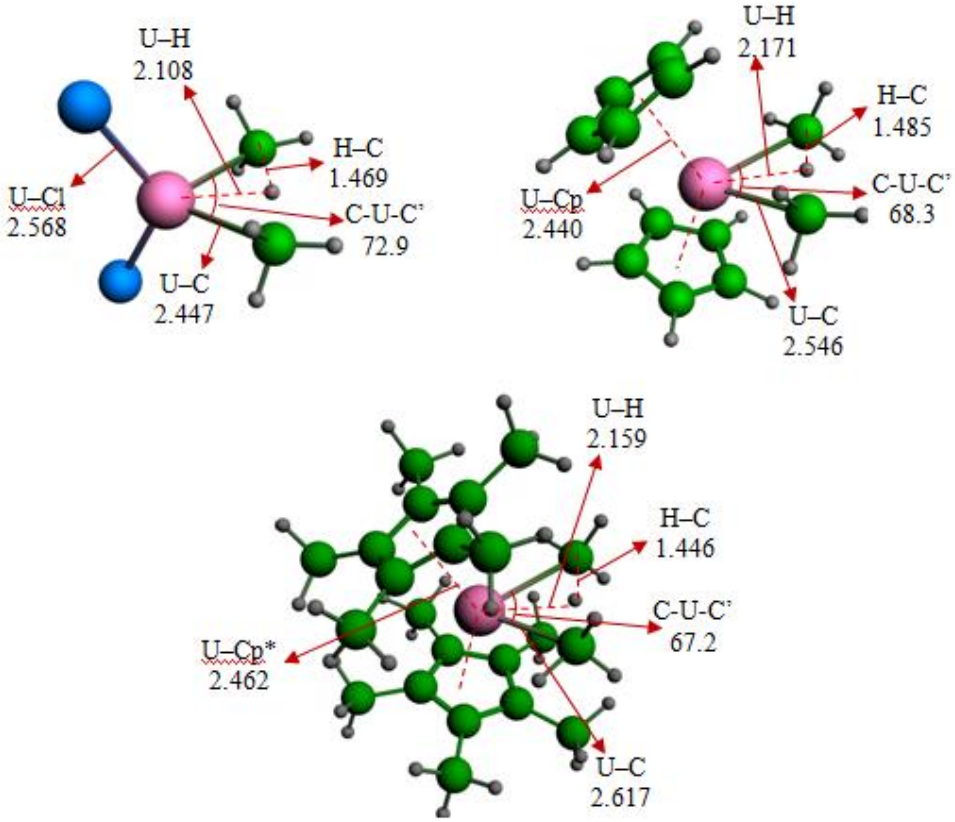


Fig.4. $L_2AnCH_3 + CH_4$ methyl exchange reaction

Whatever the actinide complex with which it reacts, the CH_4 molecule approaches the actinide atom, initiating then the formation of a bond between them; in the meantime an H atom of CH_4 moves away ending up at midway between the two CH_3 groups in the transition state.

In Figure 5 are displayed the geometries of the transition states of the $L_2UCH_3 + CH_4$ reactions (L = Cl, Cp and Cp *) given as examples.



ACCEPTED MANUSCRIPT

Fig. 5. Optimized transition states of $L_2UCH_3 + CH_4$ reactions. a) L = Cl b) L = Cp c) L = Cp*. Distances are in angstroms (Å) and angles in degrees (°).

Regarding reaction (1), in the TS of the reaction involving Np, the two calculated Np–C distances are practically the same. The Np–C bond is elongated from 2.363 Å in the free complex to 2.461 in the TS, so undergoing an increase around 0.1 Å. It was the smallest lengthening calculated in this series of reactions, just at the beginning of the bond breaking between the CH_4 molecule and the remaining complex. On the other hand, the Cl_2ThCH_3 complex has the highest C–Th bond lengthening, i.e. 0.2 Å.

The two An–Cl and An–Cl' distances do not undergo significant variations. In the Cl_2ThCH_3 complex, these distances do not change while in the complexes Cl_2UCH_3 and Cl_2NpCH_3, they lengthen by about 0.04 Å value representing the maximum calculated deviation.

At the approach of the CH_4 reactant, the Cl–An–Cl' angle opens on average about 11.4 ° in the complexes having a pyramidal geometrical structure at the beginning (cases of Ac, U, Np and Pu systems) whereas this opening is approximately close to 7° in the Th complex which presents a planar geometrical structure in the initial state.

Concerning the Cp_2AnCH_3 and $(Cp^*)_2AnCH_3$ complexes (Table3),in the TS, the Th actinide always exhibits the biggest An–C elongation which is equal to 0.19 Å and 0.2 Å respectively relatively to the ground state. The An–C(Cp) and An–C(Cp*) distances undergo only a very slight variation relatively to the reactants, not exceeding 0.03 Å. Except for Cp_2UCH_3, the Cp and Cp* ligands exhibit only a minor change of Cp–An–Cp and Cp*–An–Cp* angles equal to 6.1 °.

Table 3: Main geometrical parameters (distances (Å) and angles (°)) of the transition states of the $Cp^*_2AnCH_3 + CH_4$ reaction at the ZORA/BP86/TZP level in the gas phase

TS $(Cp^*)_2AnCH_3+CH_4$	An–Cp*	An–C	An–H	C–H	C–H–C'	C–An–C'	Cp*–An–Cp*'
Ac	2.675	2.770	2.305	1.456	175.7	63.3	140.2
Th	2.554	2.713	2.234	1.444	174.8	64.2	141.0
Pa	2.473	2.644	2.185	1.443	177.2	65.9	152.6
U	2.462	2.617	2.159	1.446	178.4	67.2	145.5
Np	2.473	2.607	2.141	1.451	177.0	67.8	139.4
Pu	2.486	2.634	2.153	1.447	176.3	66.6	134.2

It should be noted that in the Cp_2UCH_3 complex, the CH_4 approach leads to a noticeable lengthening of the U–C(Cp) bond equal to approximately 0.16 Å whereas the other U–C'(Cp)

ACCEPTED MANUSCRIPT

elongates only up to 0.07Å. On the other hand, the angle C(Cp)–U–C'(Cp') is somewhat affected by this reaction since it decreases by 13.5 °. In all the studied complexes, the proton is bridged almost halfway between the two carbons of the two methyl groups and forms an angle $C(CH_3)$–H–$C'(CH_3)$ very close to 180°, thus leading to a short An–H distance without bonding since both atoms are positively charged. The $C(CH_3)$–An–$C'(CH_3)$ angle is on average equal to 70.1°, 66.9° and 65.8° for L = Cl, Cp and Cp* respectively. This common geometrical pattern is characteristic of σ–bond metathesis that involves a proton transfer between two methyl groups and where two σ–bonds are broken and two other σ–bonds are formed simultaneously without change in the metal oxidation state contrary to oxidative addition mechanism where the metal exhibits a different oxidation state. Even if 1,2–addition mechanism shares some common features with σ–bond metathesis mechanism, it is also eliminated because it involves the π–bond participation and thus requires the presence of metal–element multiple bond. The σ–CAM involves the formation of a stable σ–complex (though not always isolable) prior to C–H cleavage which is not observed in the reactions under study.

It is also noted that the An–C and An–H distances are shorter in the Cl_2AnCH_3 + CH_4 transition state compared to its Cp and Cp* systems counterparts. In all complexes, there is a significant decrease of the An–H distance from Ac to U and U to Pu where this decrease becomes less important. On the other hand, the values of this distance in the Cp_2AnCH_3 and $(Cp^*)_2AnCH_3$ complexes are very close, as in the case of $(Cp)_2PuCH_3$ and $(Cp^*)_2PuCH_3$ where the An–H distances are 2.148 and 2.153 Å respectively whereas in Cl_2PuCH_3 this distance was found equal to 2.100 Å.

Energy profiles

These reactions correspond to a methyl exchange so that the difference in free energies between the reactants and the product is equal to zero ($\Delta G° = 0$ kcal/mol). Activation energies $\Delta G^{\#}$ were calculated as the free energy difference between the transition state and the separated reactants. The energy profiles of the activation reaction of the C–H bond of CH_4 by the complexes Cl_2UCH_3, Cp_2UCH_3 and $(Cp^*)_2UCH_3$, taken as examples, are displayed in Figure 6.

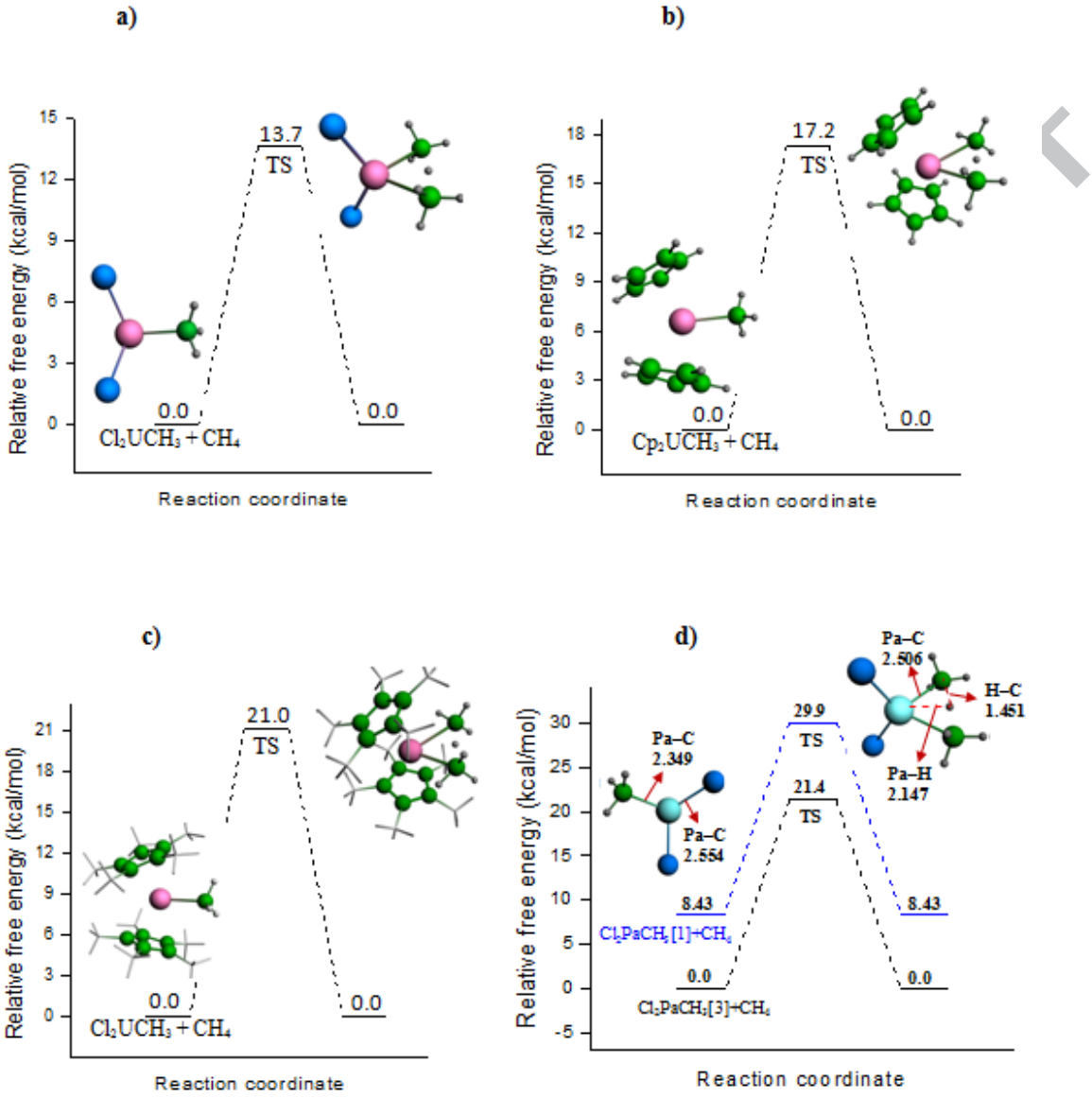


Fig. 6. Energy profiles of L_2AnCH_3 + CH_4 reactions in gas phase: a) L = Cl, An = U. b) L = Cp, An = U. c) L = Cp*, An = U. d) L = Cl, An = Pa[1] singlet and Pa[3] triplet states.

The other complexes present similar energy profiles with different activation energies $\Delta G^{\#}$, which are given in Table 4 for the three series of complexes (L = Cl, Cp and Cp*). The variations of the activation energy $\Delta G^{\#}$ as a function of the ligand are showed in Figure 7 for all complexes.

Table 4: Activation energy $\Delta G^{\#}$ (kcal/mol) of the reaction L_2AnCH_3 + CH_4 (L = Cl, Cp and Cp*) in gas phase and in THF solution (only for Cp*).

ACCEPTED MANUSCRIPT

	$\Delta G^{\#}$ (kcal/mol)			
An	L = Cl	L = Cp	L = Cp* (gas)	L = Cp* (THF)
Ac	22.92	23.42	27.32	26.93
Th	29.88	28.83	34.91	34.08
Pa	21.36	23.40	27.30	26.78
U	13.68	17.25	21.04	24.87
Np	10.48	17.10	25.13	25.25
Pu	17.51	21.11	25.03	25.79

The results show that the highest value of activation energy relative to a given series of complexes is obtained for the Th complex regardless the ligand. The Cl_2ThCH_3 and Cp_2ThCH_3 complexes have close activation energy values, i.e. 29.9 kcal/mol and 28.8 kcal/mol respectively. The activation energy of the complex $(Cp^*)_2ThCH_3$ is equal to 34.9 kcal/mol. These values show that the Th(III) complexes are the less reactive. The activation energies decrease to the lowest value by going from Th to Np in the case of Cl_2AnCH_3 and Cp_2AnCH_3 and going from Th to U in the case of the $(Cp^*)_2AnCH_3$ series of complexes. The $(Cp^*)_2UCH_3$ complex exhibits the lowest activation energy (21.04 kcal/mol) making it the most reactive among the $(Cp^*)_2AnCH_3$ series whereas Cl_2NpCH_3 and Cp_2NpCH_3 are the more reactive complexes in their corresponding series with activation energies of 10.48 and 17.10 kcal/mol respectively. Two possible spin states have been explored for the Pa complexes i.e. a triplet and a singlet one which exhibit practically identical activation energy 21.36 kcal/mol and 21.52 kcal/mol respectively for the triplet and the singlet, even if the singlet ground state of the complex is less stable by 8.43 kcal/mol relatively to the triplet one as indicated in Figure 6d.

Figure 7 shows that the two plots representing the two series of complexes Cl_2AnCH_3 and Cp_2AnCH_3 behave qualitatively in a similar way. As expected, the complexes carrying the Cp* ligands exhibit the highest activation energies due to the larger steric hindrance they create making access of the CH_4 molecule to the An–C bond difficult.

ACCEPTED MANUSCRIPT

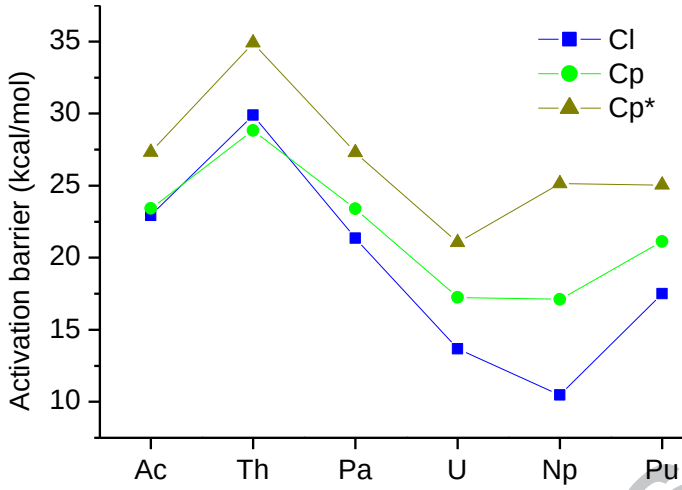


Fig. 7. Computed activation energies of the $L_2AnCH_3 + CH_4$ reactions in the gas phase

The activation energies differences between the three series of reactions ($\Delta G^{\#}(Cl) - \Delta G^{\#}(Cp)$, $\Delta G^{\#}(Cl) - \Delta G^{\#}(Cp^*)$ and $\Delta G^{\#}(Cp) - \Delta G^{\#}(Cp^*)$) have been calculated. By comparing the two sets of complexes Cl_2AnCH_3 and Cp_2AnCH_3, except Np, it is found that the ligand does not significantly affect the activation energy change since the difference calculated for each actinide complex does not exceed 3.6 kcal/mol. The Cl_2AnCH_3 and Cp_2AnCH_3 complexes with An = Ac and Th, have very close activation energies, thus when the Cl ligand is substituted by the Cp ligand, thereby indicating low steric effects within each complex due to the high distances between the metal and the ligands.

The comparison between the two series of complexes Cl_2AnCH_3 and $(Cp^*)_2AnCH_3$ shows that the difference between the activation energies increases with the decrease of the ionic metal radius and it varies between 4.4 kcal/mol for Ac and 7.5 kcal/mol for Pu. For the two series of complexes Cp_2AnCH_3 and $(Cp^*)_2AnCH_3$, this difference oscillates around the value of 3.9 kcal/mol for Ac, Pa, U and Pu and it takes the limit value of 6.1 kcal/mol in the case of Th. Methyl groups of the cyclopentadienyl rings have a more or less steric influence. However, the L_2NpCH_3 complexes (L = Cl, Cp and Cp*) remain the exception with the highest differences (6.62, 14.65 and 8.03 kcal/mol respectively).

Concerning the $(Cp^*)_2AnCH_3 + CH_4$ reaction, the influence of the solvent on the activation energies is rather weak except for the $(Cp^*)_2UCH_3$ complex which exhibits an increase of the order of 3.8 kcal/mol of the activation energy compared to the gas phase. Not surprisingly the activation energies are unaffected by the spin–orbit corrections (SOCs). In fact, according to Table 5 where the SOC energies of the different species (reactants and transition states) related to $(Cp^*)_2AnCH_3$ complexes as well as the activation energy with and

ACCEPTED MANUSCRIPT

without SOC (values within parentheses) are reported, the activation energies still have the same magnitude compared to those without SOC because both the reactants and the transition states are affected in the same way by SOC.

Table 5: Spin-orbit correction energies E_{SOC} (of reactants and transitions states) and activation energies $\Delta E^{\#}$ of $(Cp^*)_2AnCH_3$ + CH_4 reactions. (Values of $\Delta E^{\#}$ given within parentheses correspond to the activation energies without SOC); all energies are in kcal/mol.

An		Ac	Th	Pa	U	Np	Pu
E_{SOC}	Reactants	–63.88	–68.77	–86.67	102.83	–114.23	–126.59
	TS	–63.93	–68.83	–86.61	–103.09	–114.52	–126.95
$\Delta E^{\#}$		16.98 (16.91)	24.05 (24.16)	20.31 (19.76)	12.29 (12.54)	15.60 (15.85)	15.57 (15.81)

The influence of the oxidation state of the L_2AnCH_3 (L = Cl, Cp and An = Th, Pa, U, Np and Pu) reactants on their reactivity toward methane has also been studied considering the oxidation state IV which is also common to the actinides (the detailed calculations are displayed in SI.8 and SI.9). In the Cl_2AnCH_3 series of complexes, the Th and the Pa complexes still remain the less reactive but with lower barrier values, 17.4 and 14.2 kcal/mol respectively, than those with oxidation number III whereas the U, Pu and Np complexes are the more reactive with activation energies of 7.4, 10.6 and 11.8 kcal/mol respectively. In Cp_2AnCH_3 series of complexes, the trend is comparable to that of oxidation state III, the U and Np complexes are the more reactive with close activation energies (18.9 and 19.2 kcal/mol respectively) which increase slightly for Pu (19.4 kcal/mol) to Th (21.5 kcal/mol) complexes.

Charge and FMO analysis

Although the steric effects and the ionic radius of the metal cannot be neglected, these factors are not the only ones which determine the activation energies of the reaction. So, we undertook other analyses related to the transition states, the first one related to the charge distribution and transfer during the reaction process. The atomic net charges and the metal

ACCEPTED MANUSCRIPT

spin density, according to the Hirshfeld analysis, in the four centers transition state involved in the reaction are given in Table 6.

Table 6: Hirshfeld charges of TSs of the $L_2AnCH_3 + CH_4$ reaction at the ZORA/BP86/TZP level in gas phase: L = Cl (L = Cp, within parentheses).

L_2AnCH_3	Spin population	Hirshfeld net charges L = Cl (L = Cp)					
		An	Cp_2	$AnCp_2$	CH_3	CH_3'	H
Ac	0.00 (0.00)	0.84 (0.74)	–0.67 (–0.46)	0.17 (0.28)	–0.09 (–0.15)	–0.10 (–0.15)	0.01 (0.01)
Th	0.91 (1.05)	0.57 (0.56)	–0.45 (–0.33)	0.12 (0.23)	–0.07 (–0.12)	–0.07 (–0.12)	0.02 (0.02)
Pa	1.79 (2.14)	0.62 (0.66)	–0.51 (–0.46)	0.10 (0.20)	–0.06 (–0.11)	–0.06 (–0.11)	0.02 (0.01)
U	2.96 (3.19)	0.61 (0.61)	–0.54 (–0.43)	0.07 (0.19)	–0.04 (–0.10)	–0.05 (–0.10)	0.02 (0.02)
Np	4.18 (4.22)	0.60 (0.57)	–0.56 (–0.38)	0.05 (0.19)	–0.03 (–0.10)	–0.04 (–0.11)	0.02 (0.02)
Pu	5.31 (5.30)	0.74 (0.71)	–0.65 (–0.47)	0.09 (0.24)	–0.05 (–0.12)	–0.05 (–0.13)	0.01 (0.01)

The results of Table 6 show alternating positive and negative charges on the four centers involved in reactions, i.e. L_2An, CH_3, CH_3' and H, as depicted on Figure 8. This distribution of charges is likely to stabilize such transition state.

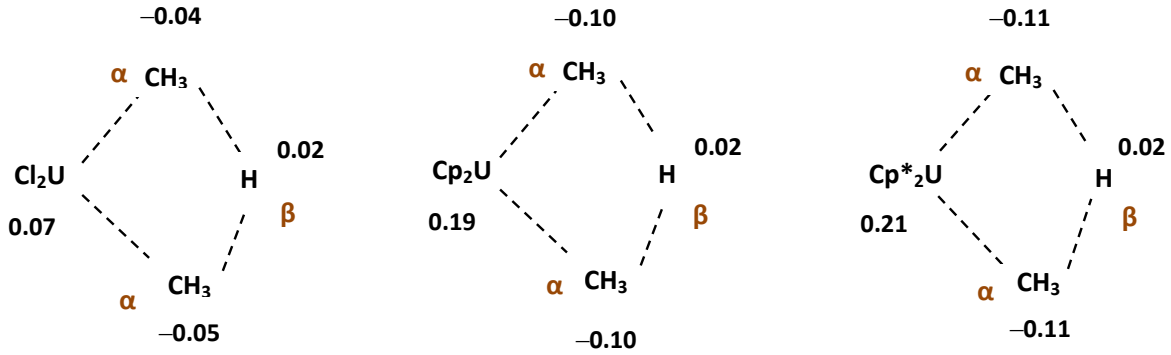


Fig. 8. Hirshfeld charge distribution in the TS structure of the $L_2UCH_3 + CH_4$ reaction (L= Cl, Cp and Cp *).

There is a significant difference in charge localization between the two sets of Cl_2AnCH_3 and Cp_2AnCH_3 complexes. The Hirshfeld charge of the Cl_2An fragment is smaller than that of the Cp_2An fragment which is itself close to that of the $(Cp^*)_2An$ fragment of the $(Cp^*)_2AnCH_3$ complex series.

ACCEPTED MANUSCRIPT

Since this is a mechanism for a proton transfer between two methyl groups, it is interesting to follow and analyze the evolution and redistribution of the electronic charges during the reaction. In the reaction whatever the ligand, the $H_3C–H$ bond approaches the An–C bond with the CH_3 group closer to the metal. The strong polarity of An–C bond induces the polarization of the $H_3C–H$ bond required for this reaction. It seems that there is no direct correlation between the charge polarity (charge separation) of the $An–C(CH_3)$ bond and the values of the calculated activation energies along each series. Moreover, a large polarity (charge separation) in the case of the Cp_2AnCH_3 and $(Cp^*)_2AnCH_3$ complexes does not necessarily lead to low activation energies.

During the reaction process the charges distribution changes; the $An–C(CH_3)$ bonds become less polarized than in the reactive state and charge transfer from the methyl group to the L_2An fragment occurs. To evaluate the influence of this evolution on the activation energies, we calculated the variations of charge *Δq (TS – reactant)* of the L_2An fragment as the difference between its charges in the TS and in the reactant (as given in Table 7).

Table 7: Hirshfeld Charge difference of the L_2An fragment between the reactant and the corresponding TS.

Cl_2AnCH_3	Ac	Th	Pa	U	Np	Pu
$\Delta q\ (Cl_2An)$	–0.10	–0.06	–0.09	–0.13	–0.15	–0.12
Cp_2AnCH_3	Ac	Th	Pa	U	Np	Pu
$\Delta q\ (Cp_2An)$	–0.06	–0.04	–0.07	–0.12	–0.10	–0.08
$Cp^*_2AnCH_3$	Ac	Th	Pa	U	Np	Pu
$\Delta q\ (Cp^*_2An)$	–0.05	–0.03	–0.04	–0.09	–0.10	–0.07

The charge difference $\Delta q(Cl_2An)$ are negative thus indicating an electron density transfer from the methyl groups to the L_2An fragment. By comparing the three series of complexes with each other, we observe a decrease in the transferred charge from the Cl ligand to the Cp* one, as seen for example in Pa complexes, where the charge transfer is 0.09, 0.07 and 0.04 with Cl, Cp and Cp* ligands respectively, thus causing the increase of activation energies when passing from Cl, Cp to Cp* ligands for each actinide.

Within each series of complexes, the U and Np complexes which are characterized by high charge transfer whatever the ligands (0.13 and 0.15 respectively for the Cl ligand) exhibit also the lowest activation energies contrarily to the Th complexes which exhibit a low charge transfer (0.04 for Cl ligand) and present high activation energy.

ACCEPTED MANUSCRIPT

However, according to the Figure 9 where the correlation between the activation energy and the charge transferred from the methyl group to the L_2An fragment (with L = Cl, Cp) is displayed, a better linear correlation is noted for the reactions involving the Cl_2AnCH_3 complexes compared to those involving the Cp_2AnCH_3. In the case of $(Cp^*)_2AnCH_3$ complexes the correlation is less good even if the Np and U complexes still remain the most reactive. This is probably due the steric hindrance effect on the activation energies.

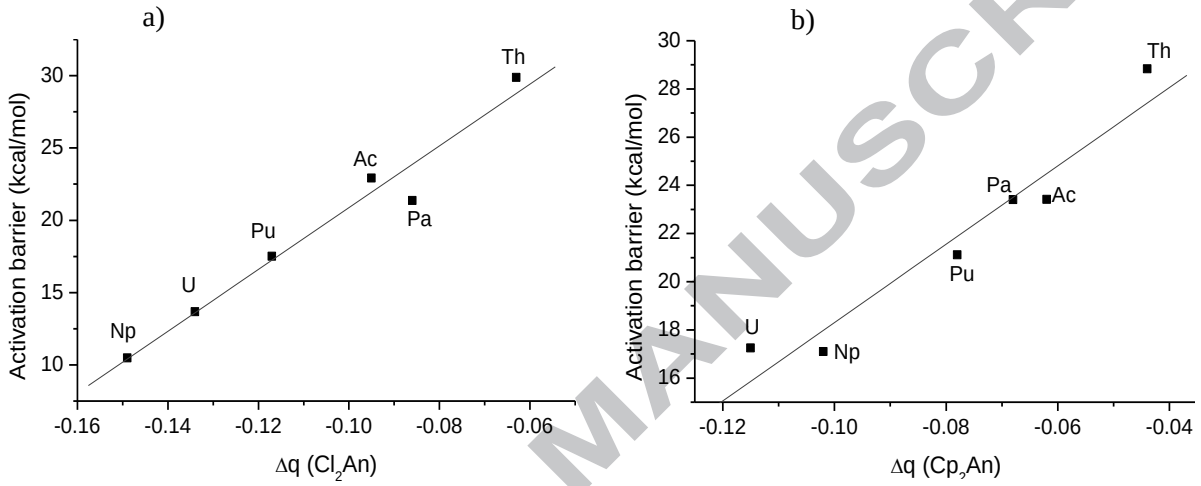


Fig. 9. Activation energy versus the transferred charges from the methyl group to the L_2An fragment $\Delta q\ (L_2An)$ for actinide complexes. a) L = Cl; b) L = Cp.

The $H–CH_3$ bond of the CH_4 reactant molecule generally becomes more polarizable in the transition state when the $L_2An–CH_3$ bond presents a polar character. The increase of the polarity of the M–C and $H–CH_3$ bonds to be activated promotes their breaking. Thus, a large polarization of the bonds has the effect of reducing the activation energy.

As suggested by Bursten and Burns [53] discussing the covalent character of An–ligand bonds for the early actinides, the actinide 6d orbitals, which are more diffuse, are involved in the covalent nature of the $An–CH_3$ bond. In addition, it is known that An 5f orbitals are less contracted compared to those of lanthanide 4f and they are also involved in the formation of covalent bonds.

Moreover, in the early actinides, the 5f orbitals are very close in energy to the 6d orbitals (more than the 4f and 5d lanthanide orbitals) and can therefore be involved with the latter orbitals and the 7s orbitals to form metal–ligand bonds. Noting that even if the contribution of 6d and 7s orbitals to the FMOs is low for the almost complexes understudy, the calculation

ACCEPTED MANUSCRIPT

shows that these atomic orbital contribute to the other inner molecular orbitals lower in energy; indeed, in the case of Cl_2PaCH_3, the percentage contributions to SOMO–1 of 7s and 6d orbitals are respectively 34.9% and 11.6% in the transition state, and of 43.3% and 24.51% in the reactant.

For the transition states of $Cl_2AnCH_3 + CH_4$ (An = Pa, U, Np and P) reactions, as one can see on Figure 10, the contribution of 5f orbitals to the SOMO are identical with a difference not more than 3.03%. The weight of these same orbitals in the LUMO is however different. It increases from Pa (78.4%) to Np (94.7%) and then decreases slightly from Np to Pu (87.7%). Here, we find that the activation energy decreases in parallel with the increase of the contribution of 5f orbitals to the LUMO.

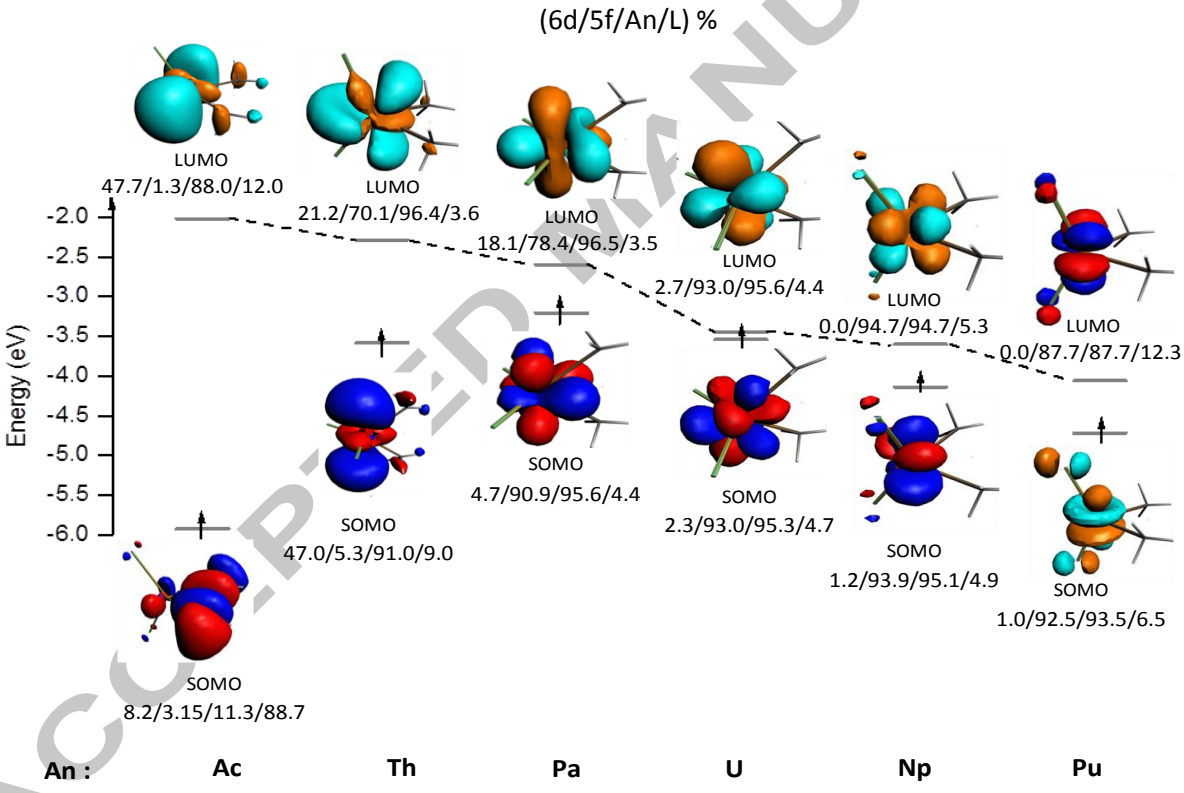


Fig. 10. Frontier Molecular Orbitals diagram of $Cl_2AnCH_3 + CH_4$ transition states at ZORA/BP86/TZP level(L% =Cl_2+CH_3).

Regarding the transition states of $Cp_2AnCH_3 + CH_4$ (An = Pa, U, Np and Pu) reactions, the contribution of the 5f orbitals to the SOMO increases from Pa (67.1%) to Np (93.5%) and then decreases from the latter to Pu (84.9 %). The involvement of 5f orbitals in the LUMO does not vary significantly for the three metals Pa, U and Np, the calculated maximum deviation does not exceed 4.4%. The contribution of Pu orbitals is lower than that of Pa by

ACCEPTED MANUSCRIPT

about 8.8%. Furthermore, we note a correlation between the activation energy and the contribution of the 5f orbitals to both SOMO and LUMO of the TSs of the $L_2AnCH_3 + CH_4$ (L = Cl and Cp); for example, the activation energies versus 5f orbitals contribution to the LUMO correlation for L = Cl is displayed in Figure 11.

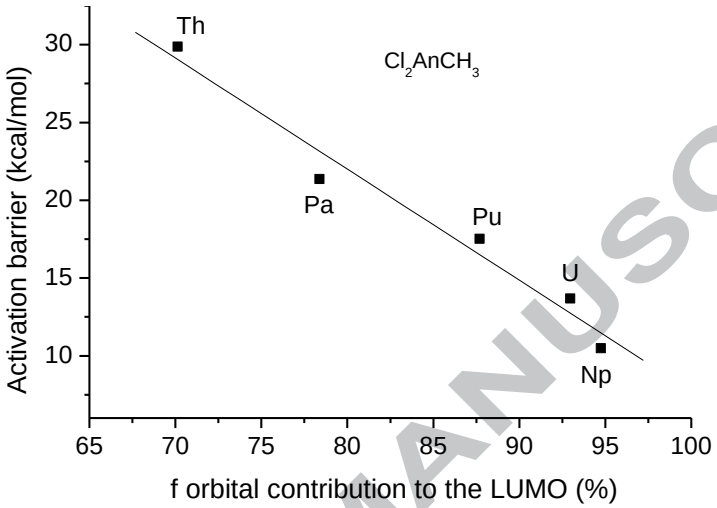


Fig. 11. Correlation between the activation energy and the contribution of 5f orbitals in LUMO (for $L_2AnCH_3 + CH_4$ reactions, L = Cl).

Thus, the transition state structures as well as the reactant complexes with mainly 5f orbitals contribution in the FMOs exhibit less important activation energies which make them more efficient to activate the methane C–H bond. In fact, the reactions involving Cl_2UCH_3 and Cl_2NpCH_3 complexes with low activation energies (13.68 and 10.48 kcal/mol respectively) correspond to the structures with an important 5f orbitals average contribution (92.9 and 94.3 % respectively) contrarily to the less reactive Cl_2ThCH_3 complex which exhibits the lowest average 5f contribution (37.7 %) in this series of complexes. The same trend is observed for the Cp_2AnCH_3 series but less pronounced in the $(Cp^*)_2AnCH_3$ series because of the steric hindrance effect which is not negligible in this case.

4. Conclusion

The present work was devoted to the study of the reactivity of L_2AnCH_3 (An = Ac, Th, Pa, U, Np and Pu; L= Cl, Cp and Cp*) complexes toward methane C–H bond activation using relativistic DFT calculations, taking into account the solvent effect and spin–orbit coupling. The computational results show that the ground state of these complexes corresponds to the

ACCEPTED MANUSCRIPT

higher spin state with mainly 5f orbital contribution to the FMO(s) in the case of Pa, U, Np and Pu complexes whatever the ligand. All the transition states found and confirmed thanks to LT and IRC calculations exhibit identical structure, four center cycles, characteristic of σ–metathesis reaction where a proton is transferred between the two methyl groups. In the two series of Cl_2AnCH_3 and Cp_2AnCH_3 complexes, the Np complex seems to be the more reactive regarding the C–H bond activation, whereas in the $Cp^*_2AnCH_3$ case, the U complex is found to be the more reactive with an activation energy of 21.04 kcal/mol; moreover, in all cases the activation energy of Np and U complexes are close. Finally, there is only a small influence of the metal oxidation state (III or IV) on the activation energies. The U(IV) and Np(IV) complexes appear to be the most reactive ones.

Charge and FMOs analyses highlight correlations between activation energies and the transferred charge from the methyl group to L_2An fragment on one hand and the weight of 5f orbitals in FMO on the other one. Globally, more important the charge transferred from the reactant CH_4 to the L_2An fragment lower is the activation energy. More important the 5f actinide orbital contribution, less important is the activation energy. Although the 6d metal orbital contribution to the metal–ligand bonding is important, the participation of the 5f electrons in bonding is evidenced particularly in the case of the two series of L_2AnCH_3 (L = Cl and Cp) complexes. This participation is also highlighted by the important 5f orbitals contribution in the FMOs. In the case of Cp* complexes, the activation energy is not only governed only by the nature of bonding but also by the steric hindrance of the Cp* ligands.

Supporting Information

SI.1: Optimized coordinates of reactants and Transition State in gas phase for: (a) $L_2AnCH_3 + CH_4$ (An = Ac, Th, Pa, U, Np, Pu) reactions; (b) $Cp_2An(Me)_2 + CH_4$ (An = U, Np) reactions.
SI.2: Optimized structures of $L_2AnCH_3 + CH_4$ systems
SI.3: Geometrical parameters of the all species (Reactants and TS) in gas phase and in THF
SI.4: Vibrational frequencies of the Transition States
SI.5: Total Bonding Energies
SI.6: Mulliken Populations, Hirshfeld Charges and Nalewajski–Mrozek bond orders Analyses
SI.7: Energies and compositions of the frontier molecular orbitals
SI.8: Optimized coordinates of $L_2AnCH_3^+ + CH_4$ systems
SI. 9: Total bonding energy of $L_2AnCH_3^+ + CH_4$ systems

ACCEPTED MANUSCRIPT

Author Information

- *Corresponding Authors*

***** E-mail:azizelkechai@yahoo.fr ; (aziz.elkechai@ummto.dz)

***** E-mail: abdou.boucekkine@univ-rennes1.fr

- *ORCID*

Aziz Elkechai:0000-0003-0808-6120

Abdou Boucekkine: 0000-0002-3714-7191

- *Notes*

The authors declare no competing financial interest.

Acknowledgements

The authors acknowledge the financial support from the Algerian Project CNEPRU n° B00L0 1501 20130025. Computing facilities were provided by ASELKAM Computer Center (UMMTO, Algeria). The authors are grateful to GENCI-IDRIS and GENCI-CINES for an allocation of computing time (Grant No. 2016-2017-080649).

References

[1] J.A. Labinger and J. E. Bercaw, Understanding and exploiting C–H bond activation, Nature, 417 (2002) 507–514.

[2] X. Jia, Z. Huang, Conversion of alkanes to linear alkylsilanes using an iridium–iron−catalyzed tandem dehydrogenation–isomerization–hydrosilylation,Nature Chemistry 8 (2016) 157–161.

[3] (a) W. Huang, P.L. Diaconescu, C–H Bond Activation of Hydrocarbons Mediated by Rare–Earth Metals and Actinides: Beyond σ–Bond Metathesis and 1,2-Addition, Advances in Organometallic Chemistry, Volume 64 (chapter two), 2015 Elsevier Inc. https://doi.org/10.1016/bs.adomc.2015.08.003; (b) W. Huang, F. Dulong, S.I. Khan, T. Cantat, P.L. Diaconescu, Bimetallic Cleavage of Aromatic C–H Bonds by Rare Earth Metal Complexes, J. Am. Chem. Soc. 136 (2014) 50, 17410–17413; (c) B.N. Williams, D. Benitez, K.L. Miller, E. Tkatchouk, W.A. Goddard, P.L. Diaconescu, An Unusual Hydrogen Migration/C–H Activation Reaction with Group 3 Metals, J. Am. Chem. Soc. 133 (2011) 4680–4683.

[4] (a) H. Schwarz, Chemistry with Methane: Concepts Rather than Recipes, Angew. Chem. Int. Ed. 50 (2011) 10096–10115; (b) H. Schwarz,P. González–Navarrete, J. Li,

ACCEPTED MANUSCRIPT

M. Schlangen, X. Sun, T. Weiske, Unexpected Mechanistic Variants in the Thermal Gas-PhaseActivation of Methane, Organometallics 36 (2017) 8–17; (c) B. Butschke, H. Schwarz, Thermal C–H Bond Activation of Benzene, Toluene, and Methane with Cationic [M(X)(bipy)]+ (M = Ni, Pd, Pt; X = CH3, Cl; bipy = 2,2′-bipyridine): A Mechanistic Study, Organometallics 30 (2011) 1588– 1598.

[5] (a) S.R. Golisz, T.B. Gunnoe, W.A. Goddard, J.T. Groves, R.A. Periana, Chemistry in the Center for Catalytic Hydrocarbon Functionalization: An Energy Frontier Research Center, Catal. Lett. 141 (2011) 213–221; (b) W.J. Tenn, K.J.H. Young, G. Bhalla, J. Oxgaard, W.A. Goddard, and R.A. Periana, C–H Activation with an O–Donor Iridium–Methoxo Complex, J. Am. Chem. Soc. 127 (2005) 14172–1417; (c) A.G. Wong–Foy, G. Bhalla, X.Y. Liu, R.A. Periana, Alkane C–H Activation and Catalysis by an O–Donor Ligated Iridium Complex, J. Am. Chem. Soc. 125 (2003) 14292–14293; (d) J.M. Gonzales, R. Distasio, R.A. Periana, W.A. Goddard, J. Oxgaard, Methylrhenium Trioxide Revisited: Mechanisms for Nonredox Oxygen Insertion in an M−CH3 Bond, J. Am. Chem. Soc.129 (2007) 15794–15804.

[6] (a) R.H. Crabtree, Alkane Carbon–Hydrogen Bond Activation, Encyclopedia of Inorganic Chemistry (2006) John Wiley & Sons, Ltd, DOI: 10.1002/0470862106.ia298 (b) M.S. Khan, A. Haque, M.K. Al–Suti, P.R. Raithby, Recent advances in the application of group–10 transition metal based catalysts in C–H activation and functionalization, Journal of Organometallic Chemistry 793 (2015) 114–133.

[7] (a)A. Yahia, L. Maron, Is Thorium a d Transition Metal or an Actinide? An Answer from a DFT Study of the Reaction between Pyridine N-Oxide and $Cp_2M(CH_3)_2$ with M = Zr, Th, and U, Organometallics 28 (2009) 672–679; (b) B.M. Gardner, P.A. Cleaves, C.E. Kefalidis, J. Fang, L. Maron, W. Lewis, A.J. Blake, S.T. Liddle, The role of 5f–orbital participation in unexpected inversion of the σ–bond metathesis reactivity trend of triamidoamine thorium(IV) and uranium(IV) alkyls, Chem. Sci. 5 (2014) 2489–2497.

[8] M. Aizenberg, D. Milstein, Catalytic Activation of Carbon–Fluorine Bonds by a Soluble Transition Metal Complex, Science 265 (1994) 359–361.

[9] (a) Y. Jin, Y. Wang, Z. Geng, H. Wang, Y. Gan, Competitive activation of C–H and C–F bonds in gas phase reaction of Ir^+ with CH3F: a DFT study, J. Organomet. Chem. 717(2012) 195–201; (b) Y. Lu, H. Sun, D. Zhang, X. Li, Theoretical study on the mechanism of selective C–F bond activation of perfluorinated toluene promoted by $Co(PMe_3)_4$, Comp. Theor. Chem. 1018 (2013) 115–119.

ACCEPTED MANUSCRIPT

[10] G.J. Kubas, Molecular hydrogen complexes: coordination of a sigma bond to transition metals, Acc. Chem. Res.21 (1988) 120–128.

[11] A.H. Janowicz, R.G. Bergman, Activation of carbon−hydrogen bonds in saturated hydrocarbons on photolysis of $(\eta^5\text{-}C_5Me_5)(PMe_3)IrH_2$,J. Am. Chem. Soc. 105 (1983) 3929–3939.

[12] S. Stahl, J.A. Labinger, Homogeneous Oxidation of Alkanes by Electrophilic Late Transition Metals, Angew. Chem. 37 (1998) 2180–2192.

[13] S. Niu, M.B. Hall, Inter- and Intramolecular C−H Activation by a Cationic Iridium(III) Center via Oxidative−Addition Reductive-Elimination and σ−Bond Metathesis Pathways, J. Am. Chem. Soc.120 (1998) 6169–6170.

[14] S.E. Bromberg, H. Yang, M.C. Asplund, T. Lian, B.K. McNamara, K.T. Kotz, J.S. Yeston, M. Wilkens, H. Frei, R.G. Bergman, C.B. Harris, The Mechanism of a C−H Bond Activation Reaction in Room−Temperature Alkane Solution, Science 278 (1997) 260–263.

[15] P. Rothwell, Carbon−hydrogen bond activation in early transition metal systems, Polyhedron 4 (1985) 177–200.

[16] D. Balcells, E. Clot, O. Eisenstein,C–H Bond Activation in Transition Metal Species from a Computational Perspective, Chem. Rev.110 (2010) 749–823.

[17] (a) K.J. de Almeida, Methane dehydrogenation by niobium ions: a first−principles study of the gas−phase catalytic reactions, Organometallics 32 (2013) 989–999; (b) F. Kias, F. Talbi, A. Elkechai, A. Boucekkine,C–F bond breaking by bare actinide monocations in the gas phase: a relativistic DFT study, Comp. Theor. Chem. 1118(2017) 133–143.

[18] P.L. Watson, Facile C–H activation by lutetium–methyl and lutetium–hydride complexes,J. Chem. Soc., Chem. Commun. (1983) 276–277.

[19] (a)B.A. Arndtsen, R.G. Bergman, T. Andrew Mobley, T.H. Peterson, Selective Intermolecular Carbon−Hydrogen Bond Activation by Synthetic Metal Complexes in Homogeneous Solution**,** Acc. Chem. Res. 28 (1995) 154–162.b) R. N. Perutz, S. Sabo–Etienne, The σ−CAM mechanism: σ complexes as the basis of σ–bond metathesis at late transition metal centers, Angew. Chem. 46 (2007) 2578−2592.

[20] E. Gretz, T.F. Oliver, A. Sen, Carbon–hydrogen bond activation by electrophilic transition–metal compounds. Palladium(II)–mediated oxidation of arenes and alkanes including methane, J. Am. Chem. Soc.109 **(**1987) 8109–8111.

ACCEPTED MANUSCRIPT

[21] R.G. Bergman. A physical organic road to organometallic C−H oxidative addition reactions, J. Organomet. Chem. 400 (1990) 273–282.

[22] L. Perrin, L. Maron, O. Eisenstein, Lanthanide complexes: electronic structure and H–H, C–H and Si–H bond activation from a DFT perspective, ACS Symposium Series 885 (2004) 116–133.

[23] L. Maron, L. Perrin, O. Eisenstein, DFT study of CH_4 activation by d^0 Cl_2LnZ (Z = H, CH_3) complexes, J. Chem., Dalton Trans. (2002) 534–539.

[24] R. Waterman,σ–Bond Metathesis: A 30–Year Retrospective**,**Organometallics32 (2013) 7249–7263.

[25] N.A. Siladke, C.L. Webster, J.R. Walensky, M.K. Takase, J.W. Ziller, D.J. Grant, L. Gagliardi, W.J. Evans**,** Actinide Metallocene Hydride Chemistry: C–H Activation in Tetramethylcyclopentadienyl Ligands to Form $[\mu-\eta^5-C_5Me_3H(CH_2)-\kappa C]^{2-}$ Tuck−over Ligands in a Tetrathorium Octahydride Complex**,** Organometallics 32 **(**2013) 6522–6531.

[26] R.G. Peters, B.P. Warner, B.L. Scott, C.J. Burns, C−H Bond Activation with Actinides: The First Example of Intramolecular Ring Bite of a Pentamethylcyclopentadienyl Methyl Group, Organometallics 18 (1999) 2587–2589.

[27] (a) P.L. Arnold, M.W. Mc Mullon, J. Rieb, F.E. Kuhn, C–H bond activation by f–block complexes, Angew. Chem. Int. Ed. 54 (2015) 82–100; (b) K.J. de Almeida, A. Cesar, Methane C–H bond activation by neutral lanthanide and thorium atoms in the gas phase: a theoretical prediction, Organometallics 25 (2006) 3407–3416.

[28] J.L. Kiplinger, B.L. Scott, E.J. Schelter, sp^3 versus sp^2 C–H bond activation chemistry of 2−picoline by Th(IV) and U(IV) metallocene complexes, Journal of Alloys and Compounds 444 (2007) 477–482.

[29] P. Yang, I. Warnke, R.L. Martin, P.J. Hay, Theoretical Studies of the sp^2 versus sp^3 C−H Bond Activation Chemistry of 2−Picoline by $(C_5Me_5)_2An(CH_3)_2$ Complexes (An = Th, U),Organometallics 27 (2008) 1384–1392.

[30] K.J. de Almeida, H.A. Duarte, Gas phase methane activation by the Ac^+–Pu^+ ions: theoretical insights into the role of 5f electrons/orbitals in early actinide chemistry, Organometallics 28 (2009) 3203–3211.

[31] P. Hohenberg, W. Kohn, Inhomogeneous electron gas, Phys. Rev. 136 (1964) 864–871.

[32] W. Kohn, L.J. Sham, Self–consistent equations including exchange and correlation effects, Phys. Rev. 140 (1965) A1133–A1138.

ACCEPTED MANUSCRIPT

[33] R.G. Parr, W. Yang, Density–Functional Theory of Atoms and Molecules, Oxford University Press, UK (1989). http://www.nrcresearchpress.com/doi/abs/10.1139/p80–159.

[34] E. van Lenthe, E.J. Baerends, J.G. Snijders, Relativistic regular two–component Hamiltonians, J. Chem. Phys. 99 (1993) 4597–4610.

[35] E. van Lenthe, E.J. Baerends, J.G. Snijders, Relativistic total energy using regular approximations, J. Chem. Phys. 101 (1994) 9783–9792.

[36] E. van Lenthe, A. Ehlers, E.J. Baerends, Geometry optimizations in the zero order regular approximation for relativistic effects, J. Chem. Phys. 110 (1999) 8943–8953.

[37] (a) A. Klamt, G. Schürmann, A new approach to dielectric screening in solvents with explicit expressions for the screening energy and its gradient, J. Chem. Soc. Perkin Trans.2 (1993) 799–805; (b) A. Klamt, V. Jones, Treatment of the outlying charge in continuum solvation models, J. Chem. Phys. 105 (1996) 9972–9981; (c) B. Delley, The conductor–like screening model for polymers and surfaces, Mol. Simul. 32 (2006) 117–123.

[38] G.C. Fonseca, J.G. Snijders, G. te Velde, E.J. Baerends, Towards an order–N DFT method, Theor. Chem. Acc. 99 (1998) 391–403.

[39] G. te Velde, F.M. Bickelhaupt, S.A.J. van Gisbergen, G.C. Fonseca, E.J. Baerends, J.G. Snijders, T. Ziegler, Chemistry with ADF, J. Comput. Chem. 22 (2001) 931–967.

[40] ADF2014.01, SCM, Theoretical Chemistry. Vrije University, Amsterdam, the Netherlands, http://www.sm.com.

[41] S.D. Vosko, L. Wilk, M. Nusair, Accurate spin–dependent electron liquid correlation energies for local spin density calculations: a critical analysis, Can. J. Chem. 58 (1990) 1200–1211.

[42] (a) A.D. Becke, Density functional calculations of molecular bond energies, J. Chem. Phys. 84 (1986) 4524–4529; (b) A.D. Becke, Density–functional exchange–energy approximation with correct asymptotic behavior, Phys. Rev. A 38 (1988) 3098–3100.

[43] (a) J.P. Perdew, Density–functional approximation for the correlation energy of the inhomogeneous electron gas, Phys. Rev. B 33 (1986) 8822–8824; (b) J.P. Perdew, Erratum for ref 30c, Phys. Rev. B, 34 (1986) 7406;(c) J.P. Perdew, Y. Wang, Accurate and simple analytic representation of the electron–gas correlation energy, Phys. Rev. B 45 (1992) 13244–13249.

[44] G. Ricciardi, A. Rosa, E.J. Baerends, S.A.J van Gisbergen, Electronic structure, chemical bond, and optical spectra of metal bis (porphyrin) complexes: a DFT/TDDFT study of the bis (porphyrin) M (IV) (M= Zr, Ce, Th) series, J. Am. Chem. Soc. 124 (2002) 12319–12334.

ACCEPTED MANUSCRIPT

[45] N. Kaltsoyannis, Recent developments in computational actinide chemistry, Chem. Soc. Rev. 32 (2003) 9–16.

[46] (a) A. Elkechai, A. Boucekkine, L. Belkhiri, M. Amarouche, C. Clappe, D. Hauchard, M. Ephritikhine, A DFT and experimental investigation of the electron affinity of the triscyclopentadienyl uranium complexes Cp_3UX, Dalton Trans. (2009) 2843–2849; (b) A. Elkechai, S. Meskaldji, A. Boucekkine, L. Belkhiri, D. Bouchet, M. Amarouche, C. Clappe, D. Hauchard, M. Ephritikhine, A relativistic DFT study of the electron affinity of the biscyclopentadienyl uranium complexes $Cp*_2UX_2$, J. Mol. Struct. (Theochem) 954 (2010) 115–123; (c) A. Elkechai, A. Boucekkine, L. Belkhiri, D. Hauchard, C. Clappe, M. Ephritikhine, Electron affinities of biscyclopentadienyl and phospholyl uranium(IV) borohydride complexes: Experimental and DFT studies, C. R. Chimie 13 (2010) 860–869.

[47] (a) A. Elkechai, Y. Mani, A. Boucekkine, M. Ephritikhine, Density functional theory investigation of the redox properties of tricyclopentadienyl–and phospholyluranium (IV) chloride complexes, Inorg. Chem. 51 (2012) 6943–6952; (b) A. Elkechai, F. Kias. F. Talbi, A. Boucekkine, Redox properties of biscyclopentadienyl uranium(V) imido–halide complexes: a relativistic DFT study, J. Mol. Model. 20 (2014) 2294–2304.

[48] C. Gonzalez, H.B. Schlegel, An improved algorithm for reaction path following, J. Chem. Phys. 90 (1989) 2154–2161.

[49] L. Castro, A Yahia, L. Maron, Are 5f Electrons Really Active in Organoactinide Reactivity? Some Insights from DFT Studies, European J. of Chemical Physics and Physical Chemistry 11 (2010) 990–994.

[50] N. Barros, D. Maynau, L. Maron, O. Eisenstein, G. Zi, R. A. Andersen, Single but stronger UO, double but weaker UNMe Bonds: The tale told by Cp_2UO and Cp_2UNR, Organometallics 26 (2007) 5059–5065.

[51] (a) R.F. Nalewajski, J. Mrozek, Modified valence indices from the two−particle density matrix, Int. J. Quantum Chem. 51 (1994) 187−200; (b) A. Michalak, R.L. DeKock, T.J. Ziegler, Bond multiplicity in transition−metal complexes: Applications of two−electron valence indices, Phys. Chem. A 112 (2008) 7256−7263.

[52] F.L. Hirshfeld, Bonded–atom fragments for describing molecular charge densities, Theor. Chim. Acta 44 (1977) 129–138.

[53] C.J. Burns, B.E. Bursten, Covalency in f–element organoletallic complexes: Theory and experiment, J. of Critical Discussion of the Current Literature 4 (1989) 61–93.

ACCEPTED MANUSCRIPT

Highlights

- Activation of C-H bond methane by actinide complexes viewed as one-proton transfer process between the two methyl's of reactants.
- Computations shows a Transition state characteristic of σ–metathesis reaction.
- High ability of uranium and neptunium complexes to activate C-H bond of methane.
- Crucial role of the 5f actinide orbitals in the lowering of the activation barriers

ACCEPTED MANUSCRIPT